

pubs.acs.org/biochemistry Article

# Kinetic Analysis of Transient Intermediates in the Mechanism of Prenyl-Flavin-Dependent Ferulic Acid Decarboxylase

April K. Kaneshiro, Karl J. Koebke, Chunyi Zhao, Kyle L. Ferguson, David P. Ballou, Bruce A. Palfey, Brandon T. Ruotolo, and E. Neil G. Marsh\*



Cite This: https://dx.doi.org/10.1021/acs.biochem.0c00856



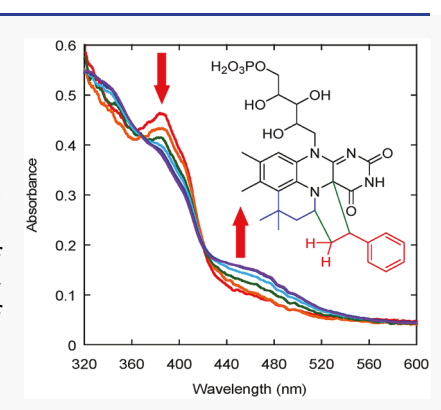
**ACCESS** 

III Metrics & More

Article Recommendations

Supporting Information

**ABSTRACT:** Ferulic acid decarboxylase catalyzes the decarboxylation of various substituted phenylacrylic acids to their corresponding styrene derivatives and  ${\rm CO_2}$  using the recently discovered cofactor prenylated FMN (prFMN). The mechanism involves an unusual 1,3-dipolar cycloaddition reaction between prFMN and the substrate to generate a cycloadduct capable of undergoing decarboxylation. Using native mass spectrometry, we show the enzyme forms a stable prFMN–styrene cycloadduct that accumulates on the enzyme during turnover. Pre-steady state kinetic analysis of the reaction using ultraviolet—visible stopped-flow spectroscopy reveals a complex pattern of kinetic behavior, best described by a half-of-sites model involving negative cooperativity between the two subunits of the dimeric enzyme. For the reactive site, the cycloadduct of prFMN with phenylacylic acid is formed with a  $k_{\rm app}$  of 131 s<sup>-1</sup>. This intermediate converts to the prFMN–styrene cycloadduct with a  $k_{\rm app}$  of 75 s<sup>-1</sup>. Cycloelimination of the prFMN–styrene cycloadduct to generate styrene and free enzyme appears to determine  $k_{\rm cat}$  for the overall reaction, which is 11.3 s<sup>-1</sup>.



**E** nzyme-catalyzed decarboxylations make up an important class of biological reactions that are ubiquitous in both primary and secondary metabolism. However, decarboxylation reactions are challenging to catalyze, as they generally possess high-energy barriers associated with the buildup of negative charge on the  $\alpha$ -carbon in the transition state. Indeed, decarboxylases catalyze some of the largest rate enhancements ( $\sim 10^{17}$ -fold) so far measured for enzymes. Therefore, nature has evolved a remarkably wide variety of catalytic strategies to facilitate decarboxylation reactions, using cofactors such as pyridoxal phosphate and thiamine pyrophosphate that serve as electron sinks, and Lewis acidic metal ions.

Decarboxylases have also attracted a growing amount of interest for their potential to function as "green" catalysts capable of catalyzing regio- and stereospecific reactions under mild conditions. Decarboxylases have been employed in engineered biosynthetic pathways designed to produce commodity chemicals such as styrene and acrylamide; bifunctional alcohols, e.g., 1,3-propanediol and 1,4-butanediol; isobutanol, which is a promising new biofuel; and high-value fine chemicals and pharmaceuticals. Importantly, under favorable conditions, decarboxylases can function as carboxylases and hydratases, leading to interest in using them for CO<sub>2</sub> capture and the hydration of double bonds to produce chiral alcohols.

Members of the newest family of decarboxylases to be discovered employ a novel modified flavin, termed prenylated FMN (prFMN), as a cofactor to effect decarboxylation reactions on otherwise unreactive aromatic substrates. <sup>10–15</sup>

prFMN contains an additional six-membered ring, appended between the C6 and N5 positions of the isoalloxazine flavin moiety, that is derived from dimethylallyl phosphate in bacteria 16 or dimethylallyl pyrophosphate in yeast. 17 This additional ring is installed by a specialized prenyl transferase enzyme. 18 Collectively, the two components of this class of decarboxylases are known as UbiD/UbiX-like decarboxylases. The canonical member, UbiD, catalyzes the decarboxylation of 4-hydroxy-3-octaprenylbenzoic acid to 2-octaprenylphenol as part of ubiquinone biosynthesis in many bacteria, whereas UbiX is the corresponding bacterial prenyl transferase. 19–21

Since their discovery, it has become apparent that UbiD/UbiX-like (de)carboxylases are widely distributed in microbes where they are involved in the metabolism of a range of aromatic polyunsaturated molecules. A recent phylogenetic analysis<sup>22</sup> identified more than 200 UbiD-like decarboxylases that fall into three subgroups: (a) phenylacrylic acid decarboxylases, of which ferulic acid decarboxylase (FDC)<sup>13,14,23</sup> is the best characterized, (b) aromatic (de)carboxylases, of which 3,4-dihydroxybenzoate decarboxylase (AroY)<sup>24</sup> is the best understood, and (c)  $\alpha$ , $\beta$ -unsaturated

Received: October 23, 2020 Revised: December 11, 2020



Figure 1. Proposed 1,3-dipolar cycloaddition mechanism of FDC. The iminium species of prFMN (species A) performs a 1,3-dipolar cycloaddition on the phenyl acrylate substrate (intermediate B), resulting in a cycloadduct (intermediate C). Decarboxylation then occurs coupled to the cleavage of the C4a–C $\beta$  bond, forming a singly tethered adduct (intermediate D). A proton is abstracted from a conserved active site glutamic acid as a second cycloadduct is formed (intermediate E). Finally, a cycloelimination reaction is performed, freeing the product styrene and re-forming the iminium form of prFMN (species F).

aliphatic decarboxylases, exemplified by tautomycetin-D decarboxylase (TtnD).<sup>22</sup> These latter enzymes are involved in secondary metabolism and make up the most recently identified subgroup.

The mechanism by which prFMN-dependent enzymes catalyze decarboxylations remains to be fully elucidated and is especially interesting because the cofactor may function by more than one mechanism. For the phenylacrylic acid and  $\alpha,\beta$ -unsaturated aliphatic decarboxylases, a mechanism involving a novel 1,3-dipolar cycloaddition between the substrate and prFMN has been proposed. This proposal has attracted considerable interest because genuine thermal pericyclic reactions are very rare in enzymes and 1,3-dipolar cycloadditions have no precedent in other enzymatic reactions. However, it seems implausible that a cycloaddition mechanism could operate for aromatic decarboxylases, because this would require breaking the aromaticity of the ring. Instead, as in the case of AroY, it appears more likely that prFMN may act as an electrophilic catalyst in these decarboxylations.

In this paper, we investigate the reaction performed by FDC, which catalyzes the decarboxylation of a range of ringsubstituted phenylacrylic acid (cinnamic acid) derivatives to produce the corresponding substituted styrene derivatives. 12,13 The proposed mechanism is shown in Figure 1. The formation of cycloaddition adducts in the mechanism is supported by crystallographic studies<sup>27</sup> of the enzyme complexes that provide evidence for the formation of various covalent adducts between prFMN and substrates or substrate analogues. Structures that are similar to those of several of the proposed intermediates depicted in Figure 1 have been determined. Another line of evidence supporting this mechanism derives from the reaction of FDC with a mechanism-based inhibitor that allowed the prFMN-inhibitor cycloadduct to be characterized by high-resolution native mass spectrometry.<sup>23</sup> Linear free energy analyses using a series of substituted phenylacrylic acid derivatives, combined with primary and

secondary deuterium kinetic isotope effect measurements, point to cycloelimination of the styrene product (intermediate E in Figure 1) as the rate-determining step in the reaction. Computational studies have provided further support of the energetic feasibility of forming cycloadducts between prFMN and phenylacrylic acid. Provided further support of the energetic feasibility of forming cycloadducts between prFMN and phenylacrylic acid.

Although there is now experimental evidence supporting the existence of some of the intermediates proposed in the mechanism of FDC, the kinetics of the reaction remain to be fully developed. Here we report pre-steady state kinetic analyses of FDC reacting with phenylacrylic acid, together with native mass spectrometry (MS) analyses of prFMN—substrate adducts. These data provide evidence for the formation and decay of the first cycloadduct in the reaction cycle and identify the kinetics of formation for the second cycloadduct that forms between styrene and prFMN, which is the intermediate that accumulates on the enzyme.

#### MATERIALS AND METHODS

**Reagents.** trans-Phenylacrylic acid,  $d_7$ -trans-phenylacrylic acid, styrene, and  $d_8$ -styrene were all purchased from Sigma-Aldrich Co. All other materials were purchased from Sigma-Aldrich Co. or Thermo Fisher Scientific Co.

**Expression and Purification of FDC.** Expression and purification of recombinant holo-FDC from *Escherichia coli* were performed as described previously. <sup>12</sup>

Native Mass Spectrometry Assay. Purified FDC was buffer exchanged into 200 mM ammonium acetate using Micro Bio-Spin 30 columns (Bio-Rad, Hercules, CA). Substrates were first dissolved in dimethyl sulfoxide (DMSO) to improve solubility. All reactions were performed in 200 mM ammonium acetate with a substrate:enzyme ratio of 5:1, and mixtures incubated on ice for 10 min before analysis. A pH of 6.6 was used for the reaction of FDC with styrene substrates, and a pH of 8 was used for phenylacrylic acid substrates.

Sample aliquots (5  $\mu$ L) were analyzed under native MS conditions<sup>30</sup> by ion mobility mass spectrometry (IM-MS) on a quadrupole ion mobility time-of-flight mass spectrometry (Q-IM-ToF MS) instrument (Synapt G2 HDMS, Waters, Milford, MA). The complex of FDC with substrate-prFMN adduct ions was generated using nanoelectrospray ionization (nESI). The initial instrument settings were set to minimize ion activation, thereby maintaining noncovalent interactions such that no significant signals were observed for free FMN-related peaks. The capillary voltage was set to 1.5 kV, and the sampling and extraction cones were set to 30 and 0 V, respectively, with a trap collision energy at 20 V. For CID experiments, the trap collision energy was increased to 100 V to dissociate the noncovalently bound substrate-prFMN adducts, giving rise to a series of substrate-prFMN adduct-derived peaks at low m/zvalues. Data were processed in Masslynx (Waters).

**Stopped-Flow Absorption Spectroscopy.** Purified concentrated FDC was stored in 50 mM potassium phosphate and 10% (v/v) glycerol (pH 7.5). A stock solution of 10 mM phenylacrylic acid was prepared in the same buffer as the enzyme and used to make more dilute phenylacrylic acid solutions for experiments. FDC was transferred into a glass tonometer and made anaerobic by cycling between evacuation and flushing with argon gas. Buffer and phenylacrylic acid solutions were transferred to glass syringes and made anaerobic by being bubbled with argon gas for 10 min before use. Styrene was added directly to a syringe of anaerobic buffer and used immediately to prevent introduction of oxygen.

A Hi-Tech Scientific KinetAsyst SF-61 DX2 stopped-flow spectrophotometer (TGK Scientific) controlled by the Kinetic Studios software package (TGK Scientific) was used for presteady state experiments. Single-wavelength absorbance traces were collected using a monochromator, whereas a chargecoupled device was used to collect absorbance spectra from 300 to 800 nm. The stopped-flow apparatus was made anaerobic by soaking the system overnight with an oxygenscrubbing solution containing  $\sim 0.1$  unit mL<sup>-1</sup> protocatechuate dioxygenase and 1 mM protocatechuate (3,4-dihydroxybenzoate) in 0.1 M potassium phosphate buffer (pH 7.0). The apparatus was rinsed thoroughly with anaerobic buffer before use. Reactions were performed at 4 °C. Time-dependent spectra were analyzed by singular-value decomposition<sup>31</sup> and modeled to calculate the spectra of reaction intermediates using KinTek Explorer (KinTek Corp.).

Data Averaging. For some stopped-flow data recorded at single wavelengths, the data were recorded under identical experimental conditions at different time scales to obtain data with high temporal resolution on the millisecond to second time scale. These data were then averaged to maximize the signal-to-noise ratio before fitting. Generally, three to five stopped-flow shots were recorded using the same conditions and time range, and the traces averaged. This process was repeated for a variety of time ranges to improve the quality of data at all times of interest. The exact time points at which the spectrometer recorded the individual data points were unique to each time scale. Therefore, the time dimension was first binned using Microsoft Excel. One hundred bins were used for each order of magnitude within the range of  $10^{-3}$  to 5 s. The absorbance values corresponding to each time were then averaged. Figure S1 shows an example of this procedure.

**Steady State Analysis.** The decarboxylase activity of FDC was measured spectrophotometrically at 304 nm to monitor the consumption of phenylacrylic acid. Reactions were

performed in 50 mM potassium phosphate and 10% (v/v) glycerol (pH 7.5) at 4 °C. Stock solutions of FDC and phenylacrylic acid were also prepared in this buffer and kept on ice to keep solution temperatures close to 4 °C. Reactions of 100 nM FDC with concentrations of phenylacrylic acid ranging from 20 to 800  $\mu$ M were carried out in triplicate. The initial velocities were fit to the Michaelis–Menten equation using KaleidaGraph 4.0 (Synergy Software).

Spectrum of FDC Reacted with Styrene. A 253  $\mu$ M solution of FDC was prepared in 50 mM potassium phosphate and 10% (v/v) glycerol (pH 7.5). The buffer was bubbled with argon gas that had been passed through a 5 M potassium hydroxide trap for ~24 h to remove dissolved CO<sub>2</sub>. A stock solution (87 mM) of styrene was prepared in DMSO. The enzyme was introduced into an aerobic cuvette, final concentration of 76  $\mu$ M, and the reaction was initiated by addition of styrene, final concentration of 870  $\mu$ M. The ultraviolet—visible (UV—vis) spectrum was recorded for a duration of 1 min using a Hewlett-Packard 8452a diode array spectrophotometer. Each reaction condition was performed in triplicate.

## RESULTS AND DISCUSSION

Reaction of FDC with Styrene. Our previous studies of the FDC reaction, employing linear free energy analysis and primary and secondary deuterium kinetic isotope effects, suggested that the rate-limiting step is likely to be the cycloelimination of the styrene-prFMN adduct, which would be expected to accumulate on the enzyme during catalysis.<sup>2</sup> To obtain more direct evidence that styrene accumulates on the enzyme, we studied the reaction of FDC with styrene in buffer that had been purged of CO<sub>2</sub> by being sparged with argon. Under these conditions, carboxylation of styrene (the reverse reaction) cannot proceed, and therefore, if stable, the prFMN-styrene adduct (intermediate E in Figure 1) should accumulate on the enzyme. As shown in Figure 2, the spectrum of holo-FDC (final concentration of 76  $\mu$ M) in degassed buffer has a clear peak at 380 nm characteristic for the prFMN iminium species. Upon addition of styrene (final concentration of 870  $\mu$ M), the intensity of the peak at 380 nm decreases along with the formation of a new, broad peak at 460 nm (Figure 2), indicating that a reaction between the prFMN and

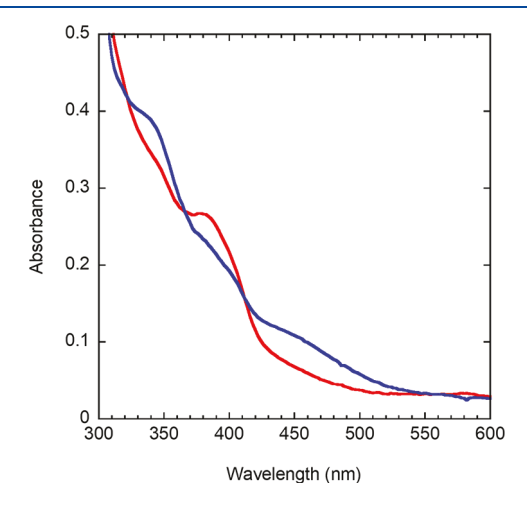


**Figure 2.** Spectral changes accompanying the reaction of prFMN with styrene. The spectrum of unreacted FDC is colored red; the spectrum of the proposed styrene adduct is colored blue.

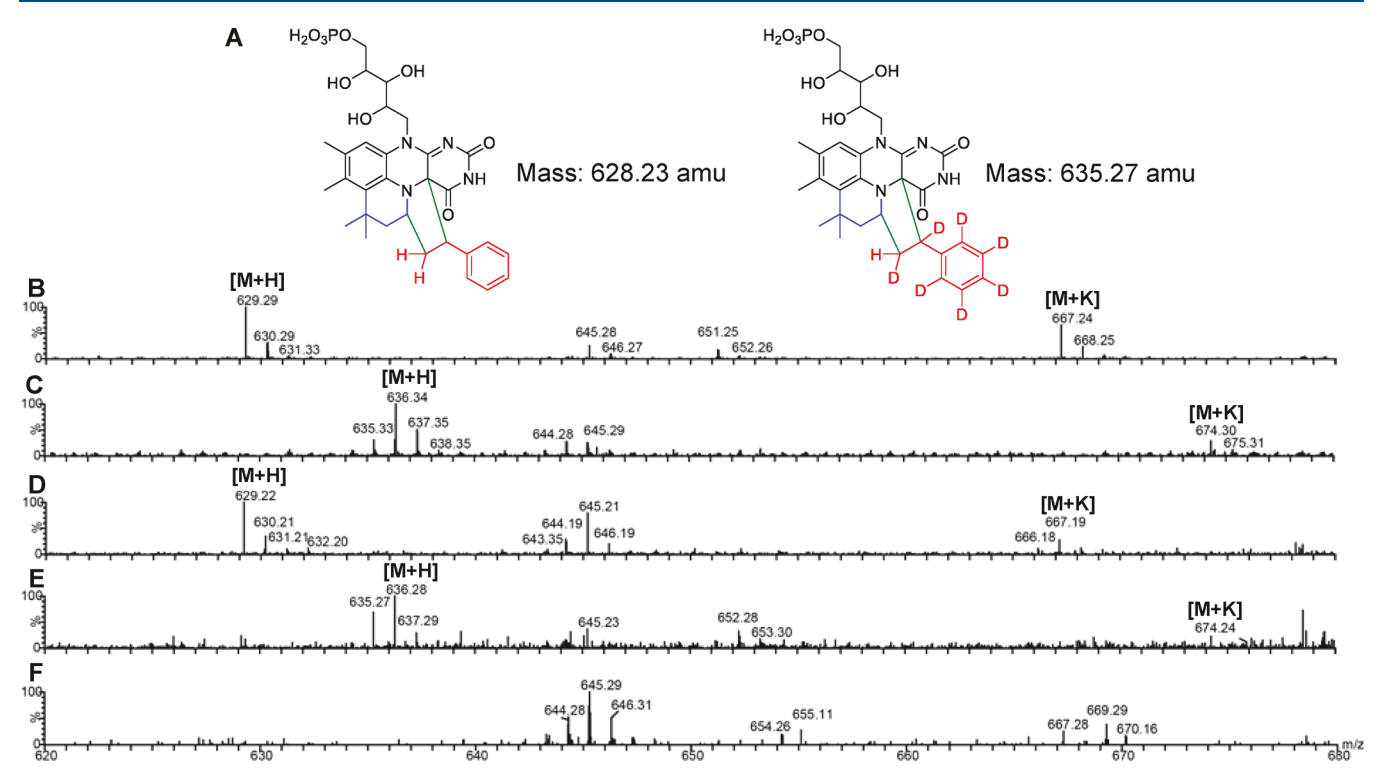


Figure 3. Identification of the prFMN-styrene cycloadduct reaction intermediate by native MS. (A) Structures of the proposed unlabeled and deuterated prFMN-styrene cycloadducts. (B) FDC reacted with *trans*-phenylacrylic acid. The peaks at m/z 629.29 and 667.24 correspond to the styrene cycloadduct complexed with a proton and a potassium ion, respectively. (C) FDC reacted with  $d_7$ -trans-phenylacrylic acid. The peaks at m/z 636.34 and 674.30 correspond to the deuterated styrene cycloadduct complexed with a proton and a potassium ion, respectively. (D) FDC reacted with styrene. The peaks at m/z 629.22 and 667.19 similarly correspond to the styrene cycloadduct complexed with a proton and a potassium ion, respectively. (E) FDC reacted with  $d_8$ -styrene. The peaks at m/z 636.28 and 674.24 correspond to the deuterated styrene cycloadduct complexed with a proton and a potassium ion, respectively. (F) Unreacted FDC. The peak at m/z 645.29, which is present in all spectra, is likely due to small amounts of a prFMN-phenylpyruvate adduct, as noted previously.<sup>13</sup>

styrene has occurred. The resulting species was stable at room temperature for several minutes. Our previous studies of FDC reacting with the mechanism-based inhibitor 2-fluoro-2-nitrovinylbenzene, <sup>23</sup> together with spectroscopic characterization of model C4a,N5-alkylated flavins, <sup>32–34</sup> which are also characterized by an absorbance band with a maximum between 425 and 460 nm, support the idea that the spectrum of FDC that had reacted with styrene represents the cycloadduct with prFMN.

Identification of prFMN Adducts by Native MS. To obtain more information about the identity of the spectroscopically observed prFMN adduct, we used native MS to characterize prFMN adducts formed by reaction with the substrate or products. Holo-FDC (20  $\mu$ M) in 200 mM ammonium acetate was incubated with either 100  $\mu$ M styrene or 20  $\mu$ M phenylacrylic acid for 10 min on ice. The protein solution was then directly introduced into the mass spectrometer. The prFMN-substrate adduct was then dissociated from the protein *in situ*, allowing the mass of the adduct to be determined before it could decompose.

The mass spectrum of the prFMN-substrate adduct (Figure 3B,D) showed two peaks at m/z 629.29 and 667.24 that matched exactly the expected values for the cycloaddition adduct of prFMN with styrene complexed with a proton and a potassium ion, respectively. These peaks were absent in control samples (Figure 3F). The same adducts were observed regardless of whether the enzyme was reacted with phenylacrylic acid or with styrene, indicating that the styrene cycloadduct is the species that accumulates on the enzyme at

equilibrium. The identity of the adduct was further confirmed when FDC was reacted with either  $d_8$ -styrene or  $d_7$ -phenylacrylic acid. In this case, the masses of the peaks due to the adduct were shifted higher by 7 amu to m/z 636.34 and 674.30 due to the presence of the deuterium label (Figure 3C,E). The loss of one deuterium atom from the adduct with  $d_8$ -styrene is explained by the enzyme-catalyzed exchange of the proton at the site of (de)carboxylation<sup>28</sup> through the transient formation of the deprotonated intermediate, D, shown in Figure 1.

Pre-Steady State Kinetic Analysis. Having established that the intermediate that accumulates on the enzyme is the cycloaddition adduct of prFMN with styrene, we proceeded to investigate the kinetics of its formation from phenylacrylic acid in more detail using stopped-flow UV-vis spectroscopy. Holo-FDC (165  $\mu$ M) was reacted with 1 mM phenylacrylic acid (final concentrations after mixing) at 4 °C in the stopped-flow spectrophotometer, and UV-vis spectra were recorded between 300 and 800 nm at various times over a period of 12.5 s. The spectra were characterized by an increase in absorbance at 460 nm and a decrease at 380 nm, indicating the accumulation of a prFMN-substrate adduct (Figure 4). After 1 s, the spectrum closely matched that of the enzyme reacted with styrene, which is consistent with the prFMN-styrene cycloadduct being the intermediate that accumulates at equilibrium. Signs of photodegradation were observed after 3 s, so in subsequent stopped-flow experiments, data collection was limited to the first two seconds of reaction.

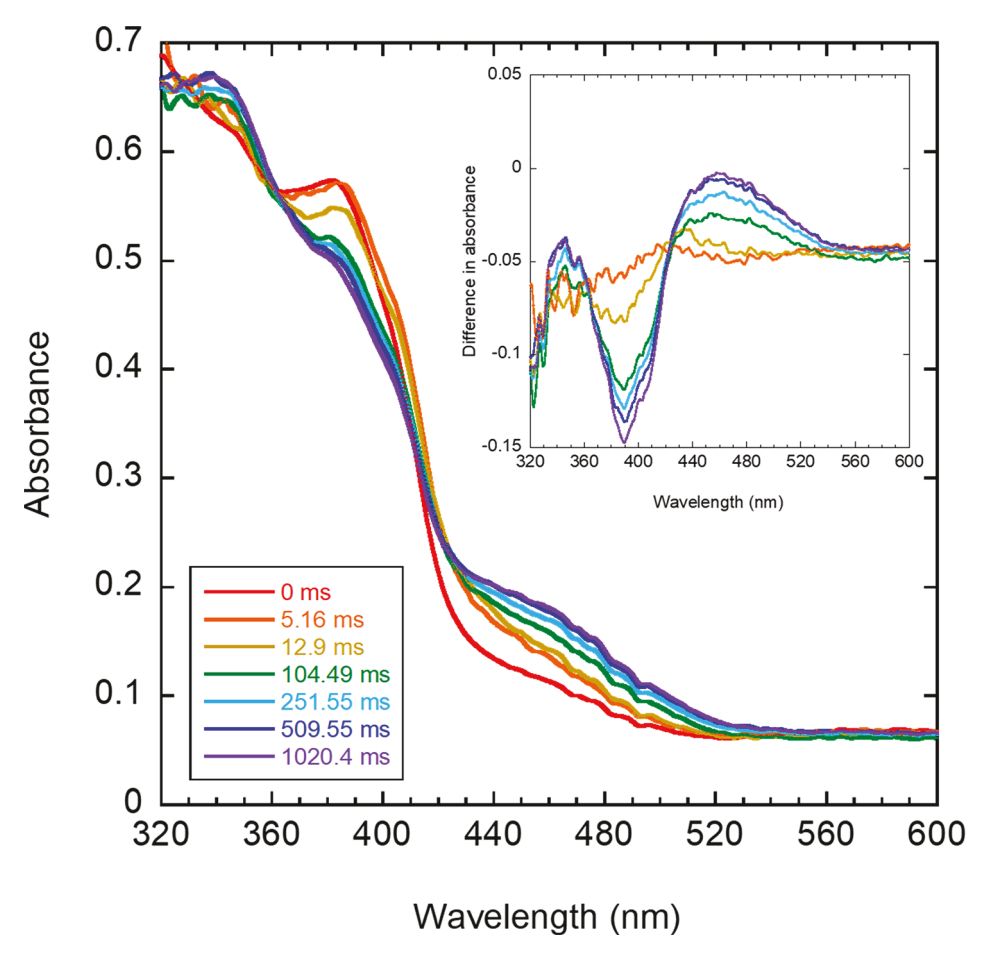


**Figure 4.** Pre-steady state spectral changes observed in reaction of FDC with phenylacrylic acid. Representative spectra shown here were recorded at times ranging from 5 ms to 1 s after mixing. The final enzyme and substrate concentrations were 165  $\mu$ M and 1 mM, respectively. The time zero spectrum was recorded by mixing FDC with buffer in the stopped-flow instrument. The inset shows difference spectra calculated by subtracting the time zero spectrum of FDC.

The steady state kinetic parameters for FDC were determined under the conditions used for the stopped-flow experiments: 4 °C in 50 mM potassium phosphate and 10% glycerol (pH 7.5). Under these conditions, the  $k_{\rm cat}$  for the decarboxylation of phenylacrylic acid was  $11.3 \pm 0.6~{\rm s}^{-1}$  and the  $K_{\rm M}$  was  $60 \pm 9~\mu{\rm M}$  (Figure S2). Therefore, in the stopped-flow experiments with the substrate in only a small molar excess over the enzyme (~6-fold), the reaction would have reached chemical equilibrium within a few turnovers and well within the initial 1 s of the experiment. This information coupled with our characterization of the styrene–prFMN cycloadduct included above indicates that this stable substrate–prFMN species is the styrene–prFMN cycloadduct.

On the basis of the spectral changes we observed in the initial experiments, we chose four wavelengths to monitor the kinetics of the reaction using monochromatic light so that photochemistry was minimized: 380 and 460 nm were selected because these wavelengths exhibited the largest absorbance changes, whereas 344 nm exhibited smaller absorbance changes. Lastly, we selected 425 nm, which from initial experiments appeared to be an isosbestic point; however, as discussed below, this is not in fact the case.

Representative traces from single-wavelength stopped-flow kinetic experiments are shown in Figure 5. At each of the wavelengths investigated, multiple kinetic phases were observed within the first second. These spectral changes are

sufficiently rapid to represent the kinetics of reactions occurring on the enzyme that are likely to be mechanistically significant. In each case, there is an initial very rapid decrease in absorbance that occurs largely within the mixing time of the spectrometer with a  $k_{\rm obs}$  of >1000 s<sup>-1</sup>. This may represent changes to the absorption characteristics of the cofactor in response to substrate binding. At slower time scales, the spectral changes depend upon the wavelength as described below.

At 380 nm, two main phases are observed that occur with  $k_{\rm obs}$  values of ~146 and ~14 s<sup>-1</sup> (Figure 5B). (We note that a further, very slow decrease in absorbance was also observed at this wavelength that required an additional exponential function to adequately fit the data. It is unclear why this occurs, but it appears to be too slow to represent catalysis.) Comparably, there are two phases observed at 460 nm characterized by similar but opposite amplitudes with  $k_{\rm obs}$  values of ~160 and ~5 s<sup>-1</sup> (Figure 5D). We consider that the biphasic increase in absorbance at 460 nm over time most likely represents the accumulation of the cycloaddition adduct between prFMN and styrene on the enzyme, which our mass spectrometry measurements and recent crystallographic studies<sup>27</sup> indicate is the enzyme species that accumulates at chemical equilibrium.

When the reaction was monitored at 344 nm, kinetic behavior similar to that observed at 460 nm was observed Biochemistry pubs.acs.org/biochemistry Article

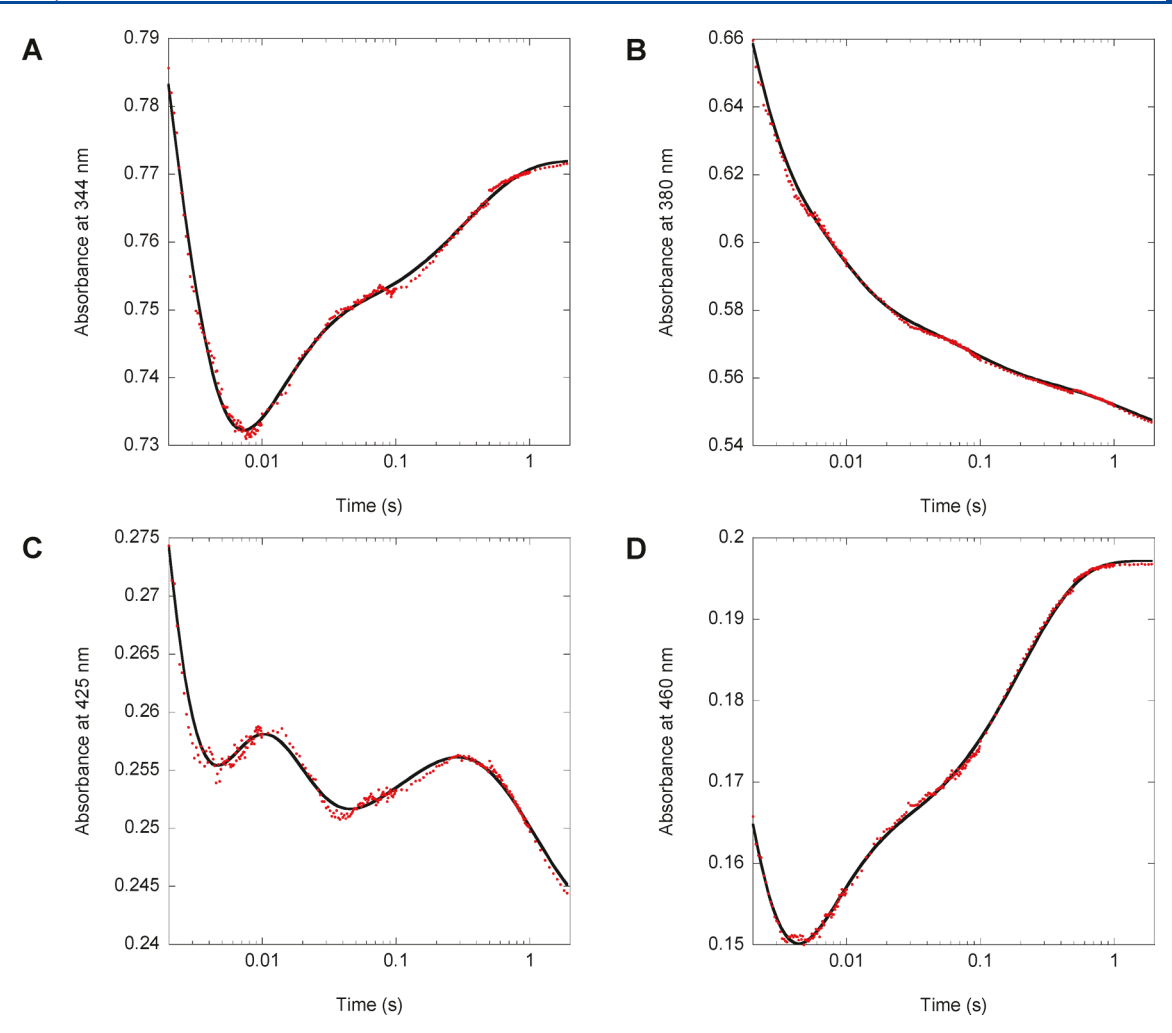


Figure 5. Pre-steady state kinetics for FDC reacting with phenylacrylic acid. The reaction of FDC (165  $\mu$ M) with phenylacrylic acid (1 mM) was monitored at four representative wavelengths, and the absorbance changes were fitted to exponential functions: (A) 344 nm, fitted to a three-exponential function, (B) 380 nm, fitted to a four-exponential function, (C) 425 nm, fitted to a five-exponential function, and (D) 460 nm, fitted to a three-exponential function. The traces shown are averaged using the procedure described in Materials and Methods. Similar fits were obtained from non-averaged data (Figure S3).

(Figure 5A). More complex kinetic behavior was observed when the reaction was monitored at 425 nm. In this case, there is an initial increase in absorbance followed by a partial decrease before a second slight increase and a final slower decrease (Figure 5C). Although the absorbance changes at these wavelengths are quite small and the data are therefore somewhat noisy, this kinetic behavior was observed over multiple shots. The apparent rate constants and amplitudes calculated from fitting these traces are listed in Table S1.

To obtain further information about this complex pre-steady state kinetic behavior, we investigated the effect of decreasing the substrate concentration on the reaction kinetics. The enzyme was reacted with 700, 500, or 150  $\mu$ M phenylacrylate (final concentrations after mixing), with the latter concentration representing an approximately stoichiometric ratio of enzyme to substrate, and the reaction was monitored at the wavelengths described above. The concentration-dependent kinetics for the reaction are shown in Figure 6, and the apparent rate constants and amplitudes calculated from fitting the kinetic traces obtained at the various wavelengths and substrate concentrations are listed in Table S1.

Although the apparent rate constants associated with the various reaction phases change little, there are marked changes

in the amplitudes associated with these phases. Notably, the amplitudes of the two slower phases are decreased, whereas the amplitudes of the two faster phases increase slightly as the substrate concentration is decreased. This effect becomes most pronounced when the substrate and enzyme are at stoichiometric concentrations and is especially evident at 425 nm (Figure 6). The concentration dependence of the reaction suggested that FDC may exhibit half-of-sites reactivity arising from negative cooperativity between the two subunits of the dimeric enzyme. Such behavior is not uncommon in oligomeric enzymes and has been well-studied in other enzymes, an example being the homodimeric enzyme thymidylate synthase. S15,36 In the case presented here, the data suggest a tighter-binding "fast" subunit and a weaker-binding "slow" subunit.

The data obtained at the various different wavelengths shown in Figure 5 illustrate the complicated nature of the kinetic behavior observed. Therefore, rather than attempt to fit the data from each specific wavelength to a kinetic model, we recorded a complete set of time-dependent spectra for the reaction of 165  $\mu$ M FDC with 1 mM phenylacrylic acid. This data set was obtained using a CCD stopped-flow spectrophotometer, and the data were subjected to global analysis using

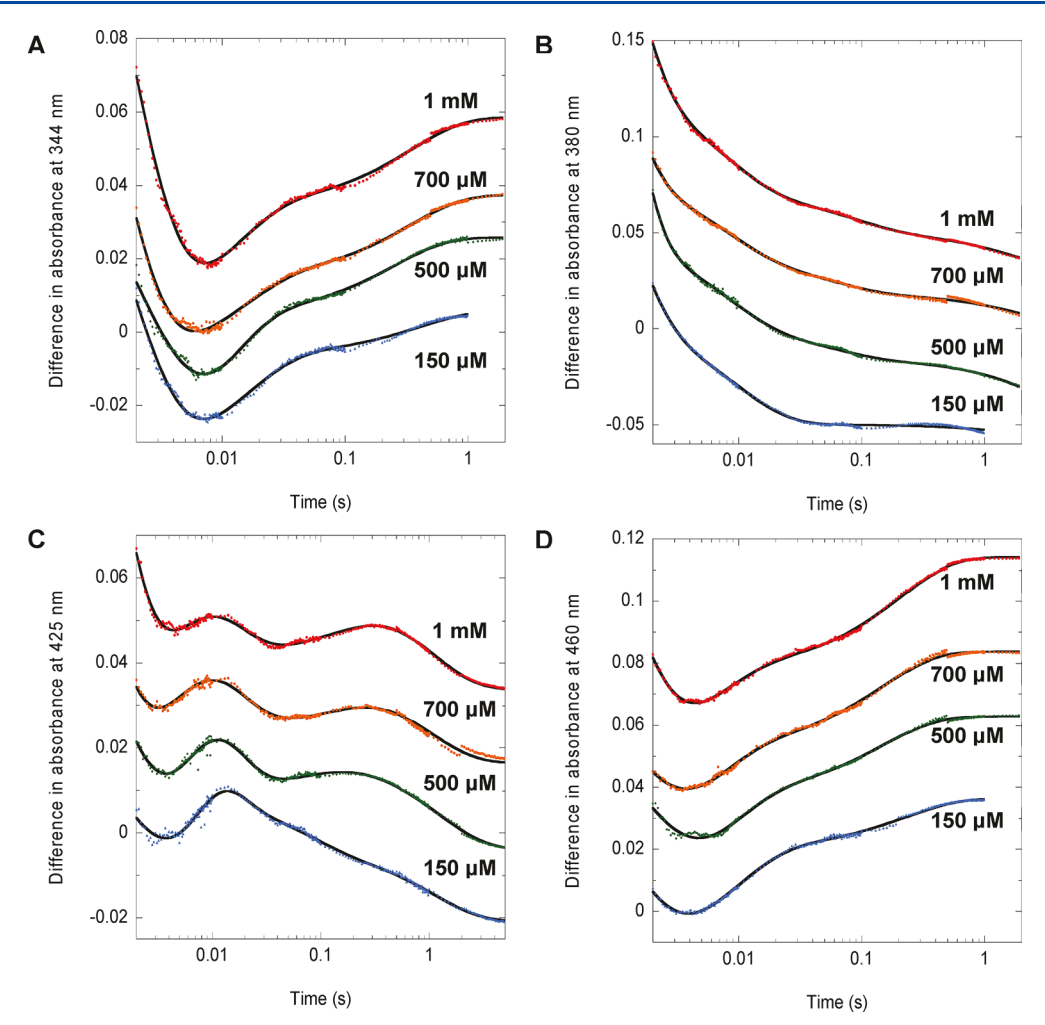
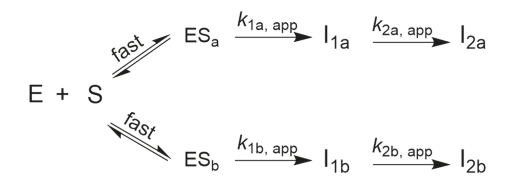


**Figure 6.** Concentration dependence of spectral changes observed for the reaction of FDC with phenylacrylic acid. The reaction of FDC (165  $\mu$ M) with the indicated concentrations of phenylacrylic acid was monitored at four representative wavelengths: (A) 344, (B) 380, (C) 425, and (D) 460 nm. The traces have been offset for the sake of clarity, and the absorbance changes were fitted to exponential functions as described for Figure 5.

Kintek Explorer. Experiments were analyzed as difference spectra by subtracting the initial spectrum at  $\sim$ 2.0 ms from each subsequent spectrum. Spectra were first filtered by singular-value decomposition<sup>31</sup> to decrease the noise, and the four most significant components (Figure S4) were used for further analysis using Kintek Explorer using the apparent rate constants estimated from fitting the single-wavelength data at 425 nm as initial values for the model.

The data were reasonably fitted by Scheme 1 that assumes rapid substrate binding and that the two active sites on the

## Scheme 1



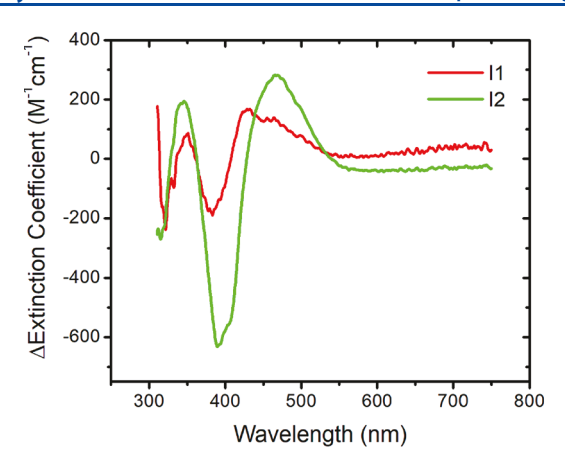
enzyme, a and b, react with different kinetics, i.e., half-of-sites reactivity. An initial, fast substrate-binding step to form the Michaelis complex on either subunit a or b of the FDC dimer is followed by two kinetically distinct steps ( $I_{1a}$ ,  $I_{1b}$ ,  $I_{2a}$ , and  $I_{2b}$  in Scheme 1) through which the Michaelis complex is

converted first to the prFMN-phenylacrylate cycloadduct and then to the final prFMN-styrene cycloadduct that accumulates on the enzyme. The choice of a mechanism with four measurable kinetic steps was dictated as the minimum needed to model the changes in the absorbance observed at 425 nm. Attempts to fit the data with fewer kinetic intermediates yielded significantly worse fits.

The apparent rate constants calculated from fitting the data to the half-of-sites model are listed in Table 1. The experimental data fit well to this kinetic model; representative fits of the model to the data at 345, 380, 425, and 460 nm are shown in Figure S5. We assumed that although the half-of-sites reactivity allowed for differing kinetic profiles between the two active sites of the FDC dimer, the spectra of the intermediates would be the same for each active site. Using this model, we

Table 1. Apparent Rate Constants Calculated from Global Fitting of Pre-Steady State Kinetic Data

| parameter                       | value (s <sup>-1</sup> ) | standard error (s <sup>-1</sup> ) |
|---------------------------------|--------------------------|-----------------------------------|
| $k_{1\mathrm{a,app}}$           | 131                      | 7                                 |
| $k_{ m 2a,app}$                 | 75                       | 4                                 |
| $k_{ m 1b,app} \ k_{ m 2b,app}$ | 4.5                      | 0.1                               |
| $k_{ m 2b,app}$                 | 0.55                     | 0.02                              |



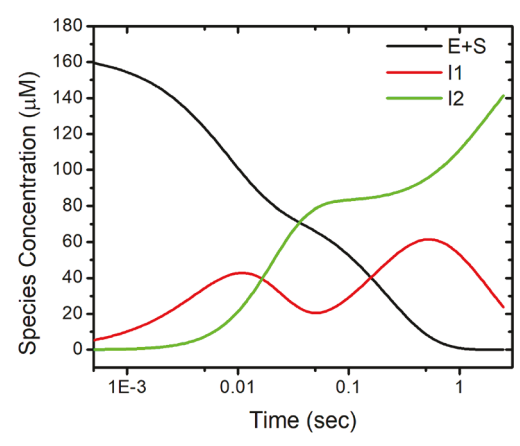


Figure 7. Global fitting of pre-steady state kinetic data for FDC reacting with phenylacrylic acid. Difference spectra (left) calculated for intermediates  $I_1$  and  $I_2$ , in Scheme 1 (a and b active sites assumed to have the same spectra). Calculated time course (right) for the accumulation and decay of reaction intermediates in Scheme 1. Data fitting performed using Kintek Explorer.

ascribe the fastest phase, described by  $k_{\rm la}$ , to the formation of the cycloadduct between phenylacrylate and prFMN (intermediate C in Figure 1) at the fast site. The slower phase described by  $k_{\rm 2a}$  is ascribed to the conversion of C to E, the prFMN–styrene cycloadduct, at the fast site. Similarly,  $k_{\rm 1b}$  and  $k_{\rm 2b}$  are ascribed to the formation of intermediate C and its subsequent conversion to E, respectively, at the slow site.

The component spectra of the intermediates calculated from global fitting are shown as difference spectra in the left panel of Figure 7. The difference spectrum of the initially formed intermediate,  $I_1$  (intermediate C in Figure 1), is distinguished by a positive absorption peak at 425 nm with a shoulder extending to  $\sim 520$  nm and a negative absorbance at 390 nm. In comparison, the later intermediate  $I_2$  (intermediate E in Figure 1) is characterized by difference spectra with a large negative peak at 390 nm and a broad positive peak at  $\sim 460$  nm. This latter spectrum matches well to the spectrum of the stable prFMN–styrene cycloadduct obtained by reaction of styrene with FDC.

The spectrum of the first intermediate to form is very similar to that of the adduct formed by reacting FDC with 2-fluoro-2-nitro-vinylbenzene, which is a mechanism-based inhibitor that mimics the structure of phenylacrylate. We previously characterized this adduct, demonstrating by native MS analysis that it reacts to form a cycloadduct with prFMN.<sup>23</sup> These observations support the idea that the transiently formed intermediate is the prFMN-phenylacrylate adduct (intermediate C in Figure 1). The spectrum is unlikely to represent the other proposed prFMN adduct, the phenylethylene adduct formed after decarboxylation (intermediate D in Figure 1), because, by analogy with the spectra of model flavin compounds, this species is expected to have absorption maxima at ~350 nm with a lower-intensity band that extends out to ~800 nm.<sup>13</sup>

The fact that the complicated spectral signature of this reaction can be modeled using three spectral components (ES,  $I_1$ , and  $I_2$ ) is consistent with our proposal for half-of-sites reactivity. Further detailed studies will be needed to elucidate the structural changes, induced substrate binding at one active site, that introduce asymmetry into FDC homodimer that, in turn, results in the two active sites having different reaction kinetics. It is worth noting that the apparent rate constant for the formation of the final intermediate ( $k_{2b} = 0.55 \ s^{-1}$ ) is an order of magnitude slower than the  $k_{\rm cat}$  of 11.3 s<sup>-1</sup> measured

under the same conditions. This observation suggests that the enzyme—prFMN—styrene cycloadduct that ultimately accumulates on the enzyme may not represent a true, kinetically competent intermediate, but rather may be a product-inhibited form of the enzyme.

# CONCLUSIONS

Here we present the first detailed kinetic analysis of a member of the recently identified and rapidly expanding family of prFMN-dependent decarboxylases. We demonstrate that the species that accumulates on the enzyme is the cycloadduct of styrene with prFMN. This implies that cycloelimination of this adduct to release the product is most likely the ratedetermining step in catalysis, consistent with our earlier Hammett analysis of FDC. 28 FDC exhibits complicated presteady state kinetic behavior that can be ascribed to half-ofsites reactivity, with one subunit of the FDC dimer reacting an order of magnitude faster than the other. These studies have allowed the apparent rate constants for the reaction of prFMN with phenylacrylate to be determined. For the fast site, formation of the initial cycloadduct of phenylacrylate with prFMN occurs with a  $k_{\rm app}$  of ~130 s<sup>-1</sup>. The conversion of this intermediate to the decarboxylated cycloadduct of prFMN with styrene occurs with a  $k_{app}$  of ~75 s<sup>-1</sup>. Finally, cycloelimination of the product and diffusion from the active site is likely the rate-determining step represented by a  $k_{\rm cat}$  of 11.3 s<sup>-1</sup>. The spectral changes described by  $k_{app}$  values of 4.5 and  $0.55~\text{s}^{-1}$  are thought to be due to reaction at the slower second subunit and appear to be too slow to be kinetically competent.

# ASSOCIATED CONTENT

# **Supporting Information**

The Supporting Information is available free of charge at https://pubs.acs.org/doi/10.1021/acs.biochem.0c00856.

Addition figures detailing data fitting and kinetic modeling and a table summarizing the rate constants measured at different substrate concentrations (PDF)

### **Accession Codes**

Ferulic acid decarboxylase 1, Q03034.

#### AUTHOR INFORMATION

#### **Corresponding Author**

E. Neil G. Marsh — Department of Chemistry and Department of Biological Chemistry, University of Michigan, Ann Arbor, Michigan 48109, United States; orcid.org/0000-0003-1713-1683; Email: nmarsh@umich.edu

#### **Authors**

April K. Kaneshiro – Department of Chemistry and Department of Biological Chemistry, University of Michigan, Ann Arbor, Michigan 48109, United States

Karl J. Koebke — Department of Chemistry, University of Michigan, Ann Arbor, Michigan 48109, United States; orcid.org/0000-0003-2198-2667

Chunyi Zhao – Department of Chemistry, University of Michigan, Ann Arbor, Michigan 48109, United States

Kyle L. Ferguson – Department of Chemistry, University of Michigan, Ann Arbor, Michigan 48109, United States

David P. Ballou — Department of Biological Chemistry, University of Michigan, Ann Arbor, Michigan 48109, United States

Bruce A. Palfey — Department of Biological Chemistry, University of Michigan, Ann Arbor, Michigan 48109, United States: Oorcid.org/0000-0001-5098-259X

Brandon T. Ruotolo – Department of Chemistry, University of Michigan, Ann Arbor, Michigan 48109, United States; orcid.org/0000-0002-6084-2328

Complete contact information is available at: https://pubs.acs.org/10.1021/acs.biochem.0c00856

#### **Author Contributions**

All of the authors contributed to the preparation of the manuscript. A.K.K., C.Z., K.L.F., D.P.B., and B.A.P. designed and conducted the experiments and analyzed the data. K.J.K. analyzed the kinetic data. C.Z. and B.T.R. designed and performed the MS experiments. A.K.K., K.J.K., and E.N.G.M. wrote the manuscript. E.N.G.M. conceptualized the idea for the manuscript. All authors reviewed the results and approved the final version of the manuscript.

#### Funding

This research was supported by National Science Foundation Grants CHE 1608553 and CHE 1904759 to E.N.G.M.

#### Notes

The authors declare no competing financial interest.

#### ABBREVIATIONS

FDC, ferulic acid decarboxylase; prFMN, prenylated flavin mononucleotide.

# **■ REFERENCES**

- (1) Miller, B. G., and Wolfenden, R. (2002) Catalytic Proficiency: The Unusual Case of OMP Decarboxylase. *Annu. Rev. Biochem.* 71, 847–885
- (2) Wolfenden, R. (2011) Benchmark Reaction Rates, the Stability of Biological Molecules in Water, and the Evolution of Catalytic Power in Enzymes. *Annu. Rev. Biochem.* 80, 645–667.
- (3) Belcher, J., McLean, K. J., Matthews, S., Woodward, L. S., Fisher, K., Rigby, S. E. J., Nelson, D. R., Potts, D., Baynham, M. T., Parker, D. A., Leys, D., and Munro, A. W. (2014) Structure and Biochemical Properties of the Alkene Producing Cytochrome P450 OleTJE (CYP152L1) from the Jeotgalicoccus sp. 8456 Bacterium. *J. Biol. Chem.* 289, 6535–6550.

- (4) Cleland, W. W. (1999) Mechanisms of Enzymatic Oxidative Decarboxylation. *Acc. Chem. Res.* 32, 862–868.
- (5) Jordan, F., and Patel, H. (2013) Catalysis in Enzymatic Decarboxylations: Comparison of Selected Cofactor-Dependent and Cofactor-Independent Examples. *ACS Catal.* 3, 1601–1617.
- (6) Keasling, J. D. (2010) Manufacturing Molecules Through Metabolic Engineering. *Science* 330, 1355–1358.
- (7) Kourist, R., Guterl, J.-K., Miyamoto, K., and Sieber, V. (2014) Enzymatic Decarboxylation—An Emerging Reaction for Chemicals Production from Renewable Resources. *ChemCatChem* 6, 689–701.
- (8) McKenna, R., Thompson, B., Pugh, S., and Nielsen, D. R. (2014) Rational and combinatorial approaches to engineering styrene production by *Saccharomyces cerevisiae*. *Microb. Cell Fact.* 13, 123–134.
- (9) Somerville, C., Youngs, H., Taylor, C., Davis, S. C., and Long, S. P. (2010) Feedstocks for Lignocellulosic Biofuels. *Science* 329, 790–792.
- (10) Leys, D. (2018) Flavin metamorphosis: cofactor transformation through prenylation. *Curr. Opin. Chem. Biol.* 47, 117–125.
- (11) Leys, D., and Scrutton, N. S. (2016) Sweating the assets of flavin cofactors: new insight of chemical versatility from knowledge of structure and mechanism. *Curr. Opin. Struct. Biol.* 41, 19–26.
- (12) Lin, F., Ferguson, K. L., Boyer, D. R., Lin, X. N., and Marsh, E. N. G. (2015) Isofunctional Enzymes PAD1 and UbiX Catalyze Formation of a Novel Cofactor Required by Ferulic Acid Decarboxylase and 4-Hydroxy-3-polyprenylbenzoic Acid Decarboxylase. ACS Chem. Biol. 10, 1137–1144.
- (13) Payne, K. A. P., White, M. D., Fisher, K., Khara, B., Bailey, S. S., Parker, D., Rattray, N. J. W., Trivedi, D. K., Goodacre, R., Beveridge, R., Barran, P., Rigby, S. E. J., Scrutton, N. S., Hay, S., and Leys, D. (2015) New cofactor supports  $\alpha,\beta$ -unsaturated acid decarboxylation via 1,3-dipolar cycloaddition. *Nature* 522, 497–501.
- (14) Piano, V., Palfey, B. A., and Mattevi, A. (2017) Flavins as Covalent Catalysts: New Mechanisms Emerge. *Trends Biochem. Sci.* 42, 457–469.
- (15) Wang, P.-H., Khusnutdinova, A. N., Luo, F., Xiao, J., Nemr, K., Flick, R., Brown, G., Mahadevan, R., Edwards, E. A., and Yakunin, A. F. (2018) Biosynthesis and Activity of Prenylated FMN Cofactors. *Cell Chem. Biol.* 25, 560–570.e6.
- (16) White, M. D., Payne, K. A. P., Fisher, K., Marshall, S. A., Parker, D., Rattray, N. J. W., Trivedi, D. K., Goodacre, R., Rigby, S. E. J., Scrutton, N. S., Hay, S., and Leys, D. (2015) UbiX is a flavin prenyltransferase required for bacterial ubiquinone biosynthesis. *Nature* 522, 502–506.
- (17) Arunrattanamook, N., and Marsh, E. N. G. (2018) Kinetic Characterization of Prenyl-Flavin Synthase from Saccharomyces cerevisiae. *Biochemistry* 57, 696–700.
- (18) Marshall, S. A., Payne, K. A. P., Fisher, K., White, M. D., Ni Cheallaigh, A., Balaikaite, A., Rigby, S. E. J., and Leys, D. (2019) The UbiX flavin prenyltransferase reaction mechanism resembles class I terpene cyclase chemistry. *Nat. Commun.* 10, 2357.
- (19) Bentinger, M., Tekle, M., and Dallner, G. (2010) Coenzyme Q Biosynthesis and functions. *Biochem. Biophys. Res. Commun.* 396, 74–79.
- (20) Gulmezian, M., Hyman, K. R., Marbois, B. N., Clarke, C. F., and Javor, G. T. (2007) The role of UbiX in *Escherichia coli* coenzyme Q biosynthesis. *Arch. Biochem. Biophys.* 467, 144–153.
- (21) Zhang, H., and Javor, G. T. (2003) Regulation of the isofunctional genes ubiD and ubiX of the ubiquinone biosynthetic pathway of *Escherichia coli. FEMS Microbiol. Lett.* 223, 67–72.
- (22) Annaval, T., Han, L., Rudolf, J. D., Xie, G., Yang, D., Chang, C.-Y., Ma, M., Crnovcic, I., Miller, M. D., Soman, J., Xu, W., Phillips, G. N., and Shen, B. (2018) Biochemical and Structural Characterization of TtnD, a Prenylated FMN-Dependent Decarboxylase from the Tautomycetin Biosynthetic Pathway. ACS Chem. Biol. 13 (9), 2728–2738
- (23) Ferguson, K. L., Eschweiler, J. D., Ruotolo, B. T., and Marsh, E. N. G. (2017) Evidence for a 1,3-Dipolar Cyclo-addition Mechanism

I

Biochemistry pubs.acs.org/biochemistry Article

- in the Decarboxylation of Phenylacrylic Acids Catalyzed by Ferulic Acid Decarboxylase. *J. Am. Chem. Soc.* 139, 10972–10975.
- (24) Payer, S. E., Marshall, S. A., Bärland, N., Sheng, X., Reiter, T., Dordic, A., Steinkellner, G., Wuensch, C., Kaltwasser, S., Fisher, K., Rigby, S. E. J., Macheroux, P., Vonck, J., Gruber, K., Faber, K., Himo, F., Leys, D., Pavkov-Keller, T., and Glueck, S. M. (2017) Regioselective para-Carboxylation of Catechols with a Prenylated Flavin Dependent Decarboxylase. *Angew. Chem., Int. Ed.* 56, 13893–13897.
- (25) Baunach, M., and Hertweck, C. (2015) Natural 1,3-Dipolar Cycloadditions. Angew. Chem., Int. Ed. 54, 12550–12552.
- (26) Pindur, U., and Schneider, G. H. (1994) Pericyclic key reactions in biological systems and biomimetic syntheses. *Chem. Soc. Rev.* 23, 409–415.
- (27) Bailey, S. S., Payne, K. A. P., Saaret, A., Marshall, S. A., Gostimskaya, I., Kosov, I., Fisher, K., Hay, S., and Leys, D. (2019) Enzymatic control of cycloadduct conformation ensures reversible 1,3-dipolar cycloaddition in a prFMN-dependent decarboxylase. *Nat. Chem.* 11, 1049–1057.
- (28) Ferguson, K. L., Arunrattanamook, N., and Marsh, E. N. G. (2016) Mechanism of the Novel Prenylated Flavin-Containing Enzyme Ferulic Acid Decarboxylase Probed by Isotope Effects and Linear Free-Energy Relationships. *Biochemistry* 55, 2857–2863.
- (29) Tian, G., and Liu, Y. (2017) Mechanistic insights into the catalytic reaction of ferulic acid decarboxylase from Aspergillus niger: a QM/MM study. *Phys. Chem. Chem. Phys.* 19, 7733–7742.
- (30) Ruotolo, B. T., Benesch, J. L. P., Sandercock, A. M., Hyung, S.-J., and Robinson, C. V. (2008) Ion mobility-mass spectrometry analysis of large protein complexes. *Nat. Protoc.* 3, 1139–1152.
- (31) Henry, E. R., and Hofrichter, J. (1992) [8] Singular value decomposition: Application to analysis of experimental data. *Methods Enzymol.* 210, 129–192.
- (32) Eckstein, J. W., Hastings, J. W., and Ghisla, S. (1993) Mechanism of bacterial bioluminescence: 4a,5-Dihydroflavin analogs as models for luciferase hydroperoxide intermediates and the effect of substituents at the 8-position of flavin on luciferase kinetics. *Biochemistry* 32, 404–411.
- (33) Ghisla, S., Hartmann, U., Hemmerich, P., and Müller, F. (1973) Studien in der Flavin-Reihe, XVIII. Die reduktive Alkylierung des Flavinkerns2); Struktur und Reaktivität von Dihydroflavinen. *Justus Liebigs Ann. Chem.* 1973, 1388–1415.
- (34) Ghisla, S., Massey, V., Lhoste, J.-M., and Mayhew, S. G. (1974) Fluorescence and optical characteristics of reduced flavines and flavoproteins. *Biochemistry* 13, 589–597.
- (35) Johnson, E. F., Hinz, W., Atreya, C. E., Maley, F., and Anderson, K. S. (2002) Mechanistic characterization of Toxoplasma gondii thymidylate synthase (TS-DHFR)-dihydrofolate reductase. Evidence for a TS intermediate and TS half-sites reactivity. *J. Biol. Chem.* 277 (45), 43126–43136.
- (36) Lee, A. L., and Sapienza, P. J. (2018) Thermodynamic and NMR Assessment of Ligand Cooperativity and Intersubunit Communication in Symmetric Dimers: Application to Thymidylate Synthase. *Front. Mol. Biosci. 5*, 47–52.